

# Successful Surgical Removal of Occult Metastases of Medullary Thyroid Carcinoma Recurrences with the Help of Immunoscintigraphy and Radioimmunoguided Surgery<sup>1</sup>

Claire de Labriolle-Vaylet, Pierre Cattan, Emile Sarfati, Michel Wioland, Claire Billotey, Claude Brochériou, Eric Rouvier, Anne de Roquancourt, William Rostène, Serge Askienazy, Jacques Barbet, Gérard Milhaud, and Anne Gruaz-Guyon<sup>2</sup>

Institut National de la Santé et de la Recherche Médicale U.339 [C. d. L-V., W. R., A. G-G.], Service de Médecine Nucléaire [C. d. L-V., S. A.], and Faculté de Médecine [G. M.], Hôpital Saint-Antoine, 75012 Paris; Service de Chirurgie [P. C., E. S.], Service de Médecine Nucléaire [C. B.], and Service d'Anatomopathologie [C. B., A. d. R.], Hôpital Saint-Louis, Paris; Service de Médecine Nucléaire, Hôpital Trousseau, Paris [M. W.]; and Immunotech SA, Marseille [E. R., J. B.], France

## ABSTRACT

Patients with recurrent or metastatic medullary thyroid carcinoma (MTC) were referred for pretargeted immunoscintigraphy (Affinity Enhancement System; AES) and radioimmunoguided surgery (RIGS). Data collected from 13 patients establish that whole-body AES immunoscintigraphy revealed metastases <360 mg and RIGS detected micrometastases (5–15 mg). All tissue samples removed by the surgeon were diagnosed by histology and immunohistochemistry of calcitonin to check the accuracy of IS and RIGS results. AES immunoscintigraphy is very sensitive. Of 34 metastases or recurrences detected, 22 had escaped physical examination or conventional imaging. The accuracy of RIGS was 86%, its sensitivity 75%, and its specificity was 90% ( $n = 208$ ). IS and RIGS detected occult tumors that would have escaped surgery, clearly demonstrating clinical benefit. Serum calcitonin (normal, 10 pg/ml) and carcinoembryonic antigen (normal, 5 ng/ml) of two patients were restored to normal. In patients whose tumors were discovered, progression of their disease was slowed, as evidenced by the large decrease in serum calcitonin and carcino-

bryonic antigen, an important prognostic factor. Surgery was canceled in one case where IS detected distant metastases out of surgical reach. Thus, AES immunoscintigraphy and RIGS might be of valuable help for the surgical management of medullary thyroid carcinoma.

## INTRODUCTION

MTC<sup>3</sup> is treated by total thyroidectomy and bilateral lymph node ablation (1–4). The most important factor influencing prognosis is the stage of the disease recognized at diagnosis and the completeness of initial tumor resection (1, 5). Because of late diagnosis, particularly for sporadic MTC, recurrences occur in a number of cases (6, 7). Under basal conditions and after pentagastrin stimulation, circulating plasma calcitonin is the marker of MTC (8, 9). It roughly reflects tumor mass and allows an accurate assessment of the surgical treatment and an early diagnosis of relapse (6–13). The management of patients with metastatic MTC is primarily surgical, and patients with occult metastatic MTC (high plasma calcitonin without detected tumor) pose an unsolved problem (3). Thus, improved metastasis detection could advance the fight against residual disease.

Circulating CEA fails to correlate with tumor burden and is often within normal range. Rising CEA, however, has been associated with poor prognosis (3, 14). In most cases, MTC cells express high levels of CEA at their surface and technetium-99m- or indium-111-labeled monoclonal antibody or antibody fragments specific for CEA have been used in clinical studies for radioimmunodetection and radioimmunotherapy (15, 16). We used indium-111-labeled bivalent haptens targeted to cancer cells by means of bispecific antibodies, a technique referred to as the AES, which has been shown to be very effective in the detection of CEA-expressing tumors and particularly MTC (17–19). The present study establishes the usefulness of AES immunoscintigraphy and RIGS in the surgical removal of very small tumor metastases in patients with suspected occult metastases. Accuracy of immunoscintigraphy and RIGS results was checked by histology and immunostaining of tissue samples removed by the surgeon.

## PATIENTS AND METHODS

**Patients.** The protocol was approved by the local ethical committee, established by French Clinical Trial legisla-

Received 5/25/99; revised 10/25/99; accepted 11/9/99.

The costs of publication of this article were defrayed in part by the payment of page charges. This article must therefore be hereby marked *advertisement* in accordance with 18 U.S.C. Section 1734 solely to indicate this fact.

<sup>1</sup> Supported in part by Grant 6073 from the Association pour la Recherche contre le Cancer.

<sup>2</sup> To whom requests for reprints should be addressed, at Faculté de Médecine Saint-Antoine, INSERM U.339, 27 Rue Chaligny, 75012 Paris, France. Phone: (33)-1-40-01-14-66; Fax: (33)-1-43-43-89-46; E-mail: gruaz@adr.st-antoine.inserm.fr.

<sup>3</sup> The abbreviations used are: MTC, medullary thyroid carcinoma; CEA, carcinoembryonic antigen; AES, Affinity Enhancement System; RIGS, radioimmunoguided surgery; CT, computed tomography; HAMA, human antimouse antibody; di-DTPA-TL, *N*- $\alpha$ -DTPA-tyrosyl-*N*- $\epsilon$ -DTPA-lysine; % ID, percentage of injected dose.

Table 1 Patients, indications, and protocol

Patient no.	Sex	Body weight (Kg)	Indication <sup>a</sup>	Injected dose <sup>b</sup> MBq	Delay antibody/ <sup>111</sup> In-tracer (days)	Delay <sup>111</sup> In-tracer/RIGS (days)
1	F	78	A	133	3	4
2	F	76	A	215	4	3
3	F	68	B	178	5	2
4	M	70	B	148	3	4
5	F	53	B	326	4	3
6	F	66	B	303	3	2
7	F	65	C	263	4	ND <sup>c</sup>
8	F	62	C	118	5	2
9	F	64	C	155	4	3
10	F	50	C	303	4	3
11	F	40	C	157	4	3
12	M	83	C	173	4	3
13	F	55	B	178	4	3

<sup>a</sup> For each patient, the presence of unknown metastases was suspected: A, patients submitted to first surgery for thyroidectomy and bilateral lymph node dissection; B, second surgery in the absence of previous bilateral lymph node dissection; and C, surgery when bilateral lymph node dissection was performed during the first surgery.

<sup>b</sup> The bispecific antibody dose was 0.1 mg/kg body weight.

<sup>c</sup> ND, not done.

tion. Thirteen MTC patients with elevated circulating calcitonin (range, 59–36073 pg/ml; normal, <10 pg/ml) were included in the study (Table 1). CEA level was elevated for each patient (range, 7–131 ng/ml; normal, <5 ng/ml), except for patient 5. The selection criterion was the suspicion of occult metastases of MTC. Patients were considered eligible when no tumor site was found by preoperative check-up, which included: physical examination; chest X-ray; cervical and hepatic ultrasonography; cervical, thoracic, and hepatic CT scan; or when the tumor sites known before immunoscintigraphy were too small to account for the calcitonin level. Patients had had different previous treatment at various hospitals in France and Italy as indicated in Table 1. They were included because of a suspicion of occult metastases (high plasma calcitonin). Circulating calcitonin and serum CEA levels were measured by immunoradiometric assays (ELSA HCT and ELSA2 ACE, respectively; Cis Biointernational, Gif s/Yvette, France). Because the ELSA-HCT test detects picogram amounts of basal calcitonin, the pentagastrin-stimulated calcitonin level was determined for patients with normal CT levels only. Stimulated calcitonin was measured 5 min before and 0, 3, and 5 min after an infusion of pentagastrin (0.5 µg/kg; normal, peak <30 pg/ml). Circulating calcitonin and CEA follow-up after immunoscintigraphy and RIGS was terminated after any additional treatment (chemotherapy or radiotherapy) was performed. Preexisting circulating HAMA was undetectable in all patients, as assessed by a specific immunoradiometric assay (Ref. 19; sensitivity, 0.06 µg/ml).

**Tracer Synthesis and Radiolabeling.** The bivalent hapten di-DTPA-TL was synthesized as described (17, 20). di-DTPA-TL (0.1 mg per kg of body weight) in solution in 0.1 M sodium acetate, 10 mM citrate buffer (pH 5.0) was added to <sup>111</sup>InCl<sub>3</sub> (Mallinkrodt, France). For six patients, 370 MBq were used, and 185 MBq were used for seven patients. Chelation proceeded overnight at room temperature. Then, 300 µl of nonradioactive InCl<sub>3</sub> (22 µg/ml in the same acetate, citrate

buffer) were added and allowed to saturate free DTPA groups for 1 h at room temperature.

The immunoreactivity of the tracer was determined by incubating trace amounts of <sup>111</sup>In-labeled di-DTPA-TL in anti-DTPA-indium antibody-coated tubes. Consistently high immunoreactivity (96.5 ± 2.8%) permitted us to use the labeled hapten without purification.

**Antibodies and Bispecific Antibody.** The anti-CEA × anti-DTPA-indium bispecific antibody was prepared by chemical coupling of the Fab fragment of the 73A.19.22 antibody (a monoclonal IgG<sub>1,λ</sub> with specificity to the DTPA-indium complex) to the reduced Fab' of the F6 antibody (a mouse IgG<sub>1,κ</sub>, specific for human CEA; Ref. 20). This antibody is not cross-reactive with NCA.<sup>4</sup>

**Injection Protocol.** di-DTPA-TL and bispecific antibody were provided by Immunotech Pharma S.A. (Marseille, France). The bispecific antibody dose (0.1 mg/kg of body weight) was administered to patients as a 30-min i.v. infusion at 4 ± 1 days before tracer injection. At day 0, the <sup>111</sup>In-labeled di-DTPA-TL tracer (118–370 MBq) was delivered i.v.

Serum samples were collected before bispecific antibody injection and 0.08, 0.5, 1, 5, 24, and 48 h after tracer injection. Urine was collected from 0 to 5, 5 to 24, and 24 to 48 h.

**Imaging Protocol.** Whole-body scan and anterior, posterior, and lateral neck and thorax imaging were performed at 5 and 24 h after tracer injection (late images were recorded when necessary) using a large field of view tomographic camera (ADAC; Genesys) tuned to the 173 and 247 keV γ ray peaks of <sup>111</sup>In with a 20% window on each peak. The scanning speed was 12 cm·mn<sup>-1</sup> for whole-body scans, and a preset count of 400,000 counts was used for views of the neck and thorax. If necessary, single photon emission computed tomography was performed with the same camera in stepwise mode (64 frames of

<sup>4</sup> Unpublished results.

Table 2 Comparison of AES immunoscintigraphy and conventional check-up results<sup>a</sup>

Patient no.	Site	Tumors detected by classical pre-operative check-up: <sup>b</sup>			Tumors detected by immunoscintigraphy	Classical preoperative check-up score <sup>c</sup>	Immunoscintigraphy score <sup>d</sup>
		P	US	CT-Scan			
1	Thyroid	1	1	ND	1	1 TP	1 TP
2	Thyroid	1	1	ND	1	1 TP	1 TP
3	Left neck	0	0	0	2	2 FN	2 TP
4	Right neck	0	0	0	1	1 FN	1 TP
	Left neck	0	0	0	1	1 FN	1 TP
	Pretracheal	0	0	0	1	1 FN	1 TP
	Right thorax	0	ND	0	1	1 FN	1 TP
6	Right neck	1	1	1	5	1 TP 3 FN 1 ND	4 TP 1 ND
	Thyroid area	0	0	0	1	1 FN	1 FP
	Pretracheal	0	1	1	1	1 TP	1 TP
7	Left neck	0	1	ND	1	1 TP	1 TP
	Iliac bone	0	ND	0	2	2 FN	2 TP
8	Right armpit	1	1	1	1	1 TP	1 TP
9	Left neck	0	1	ND	1	1 TP	1 TP
	Thorax	0	ND	0	1	1 FN	1 TP
10	Left neck	0	1	ND	1	1 TP	1 TP
	Right neck	0	0	ND	2	2 FN	2 TP
	Pretracheal	0	0	ND	1	1 FN	1 TP
	Right mediastinum	0	ND	ND	1	1 FN	1 TP
11	Left neck	1	ND	ND	0	1 FP	1 TN
	Liver	0	2	0	>8	2 TP 6 FN	>8 TP
12	Left neck	0	2	ND	2	2 TP	2 TP
	Sus clavicular right	0	0	ND	1	1 TN	1 FP
13	Thyroid	0	1	1	0	1 FP	1 TN

<sup>a</sup> This table summarizes the number of tumors detected before surgery by conventional check-up and those visualized by immunoscintigraphy (no tumor site was detected before surgery for patient n° 5).

<sup>b</sup> P, physical examination, US, ultrasonography; CT-scan, tomodensitometry.

<sup>c</sup> TP, true-positive; TN, true-negative; FP, false-positive; FN, false-negative; ND, not done.

<sup>d</sup> Final diagnosis established on pathological examination of surgical samples or of biopsy specimen (patient 7, iliac bone; patient 11), or colioscopy (patient 11), or selective venous catheterization (patient 7, neck).

45 s over 360°). For three patients, control images were recorded after surgery.

Scan interpretation was performed by two independent experienced observers unaware of conventional imaging results. Interpretations were then compared with pathological results on surgical or biopsy specimens or for one patient (no. 7) to circulating calcitonin determination in samples obtained by selective venous catheterization.

**Radioimmunoguided Surgery.** Surgery was performed  $3 \pm 1$  days after tracer injection. The surgeon explored the operative field with a sterile hand-held gamma probe (Scintiflex, Novelec, France; Refs. 21 and 22). For each measurement, normal tissue was counted (five times, 5–10 s) in the vicinity as a reference. The signal was considered positive when the mean radioactivity counts ( $n = 5$ ) were greater than mean reference counts plus twice the SD (*i.e.*, the square root of the reference counts). The location of positive signals originating from small lymph nodes embedded in large negative tissue areas was marked with a thread to correlate precisely the pathological results with the radioactive signals. Each lymph node and surrounding tissue were removed and analyzed by the pathologist as described below. The hand-held gamma probe counts were recorded and compared with the results of pathological exami-

nation. *Ex vivo* gamma probe counts were performed on 37 locations.

**Pathological Examination.** For each tissue specimen, the tumor size was measured by the pathologist, enabling us to calculate the volume and to estimate tumor weight. Every specimen was evaluated histologically by multiple sections. Histological stains used included H&E. Immunohistochemical analysis included use of monoclonal antibodies to cytokeratin (KL1; Immunotech), to calcitonin (Dako), to CEA (Dako; CEA specific), and to CD68 (Kp1; Dako) to detect histiocytes-macrophages.

**Pharmacokinetics and Biodistribution.** Plasma and surgical sample radioactivity was measured and corrected for the physical decay of the isotope. Biexponential curves of the general formula  $[(1/V1 - 1/V2)2^{-t/T\alpha} + (1/V2)2^{-t/T\beta}]$  were fitted to individual plasma radioactivity data by nonlinear least-square regression. After weighing the surgical samples, the fraction of injected dose accumulated per gram of tissue was determined.

## RESULTS

### Tolerance to Hapten and Antibody Injection

No adverse effect was recorded during or after the injection of the bispecific antibody or of the hapten. Six patients of 13

developed antibodies directed to the murine bispecific antibody (HAMA).

### Pharmacokinetics

For all patients who underwent a first immunoscintigraphy,  $^{111}\text{In}$ -labeled di-DTPA-TL serum pharmacokinetics fitted a biexponential curve. The first half-life  $T\alpha$  was  $0.48 \pm 0.16$  h, and the second half-life  $T\beta$  was  $21.4 \pm 6.3$  h ( $n = 10$ ). Distribution volumes were, respectively:  $V1$ ,  $4.3 \pm 1.0$  liters; and  $V2$ ,  $8.8 \pm 2.0$  liters ( $n = 10$ ). The excretion of excess activity was fast; the fraction of injected dose recovered in the urine amounted to  $32 \pm 7\%$  within 5 h,  $51 \pm 6\%$  within 24 h ( $n = 11$ ), and  $57 \pm 3\%$  within 48 h ( $n = 5$ ).

### Biodistribution

The amount of radioactivity targeted to tumors was assessed in samples containing 66–100% tumor cells and expressed as a percentage of the injected dose/kg (% ID/kg) of tumor after correction for radioactive decay. The mean value for 16 samples from six patients was  $28 \pm 16\%$  ID/kg; individual values ranged from 9 to 70% ID/kg. Tumor:normal tissue contrast ratios at the time of surgery were  $13 \pm 7$  (tumor:blood),  $31 \pm 13$  (tumor:muscle), and  $28 \pm 15$  (tumor:normal lymph node).

### Comparison between Classical Preoperative Check-Up and Immunoscintigraphy Results

The 13 patients were referred for AES immunoscintigraphy with a delay of  $4 \pm 1$  days between bispecific antibody and tracer injection. Whole-body scan and anterior, posterior, and lateral neck and thorax planar imaging were performed at 5 and 24 h after tracer injection (late images were recorded when necessary). The sites of activity uptake and the sites detected by the preoperative check-up are summarized in Table 2. All sites but two (as indicated in Table 2) were checked by histology and immunostaining of calcitonin (as described in "Patients and Methods"). A typical whole-body scan (patient 3) is shown on Fig. 1. Each detected site was visualized on planar images; when necessary, the spatial location was assessed by single photon emission computed tomography.

**Tumors Detected by Conventional Imaging.** In nine patients, physical examination or conventional imaging detected 12 true-positive tumors, all of which were visualized by AES immunoscintigraphy (patients 1, 2, and 6–12; Table 2). In patient 13, echography and CT scan detected one false-positive site in the thyroid area, as assessed by the pathological examination. It was a true-negative site with AES immunoscintigraphy.

**Occult Tumors Revealed by AES Immunoscintigraphy.** AES immunoscintigraphy revealed 22 occult metastases that had escaped conventional imaging (seven patients, nos. 3, 4, 6, 7, and 9–11). For patients 3 and 4, no tumor had been in evidence in any site by the preoperative conventional imaging evaluation; AES immunoscintigraphy detected two metastases in patient 3 and four in patient 4 (because images of the thorax at 24 h were doubtful for patient 4, additional images were recorded at 72 h, which confirmed one of the four radioactivity accumulation sites corresponding to a metastasis). The recur-

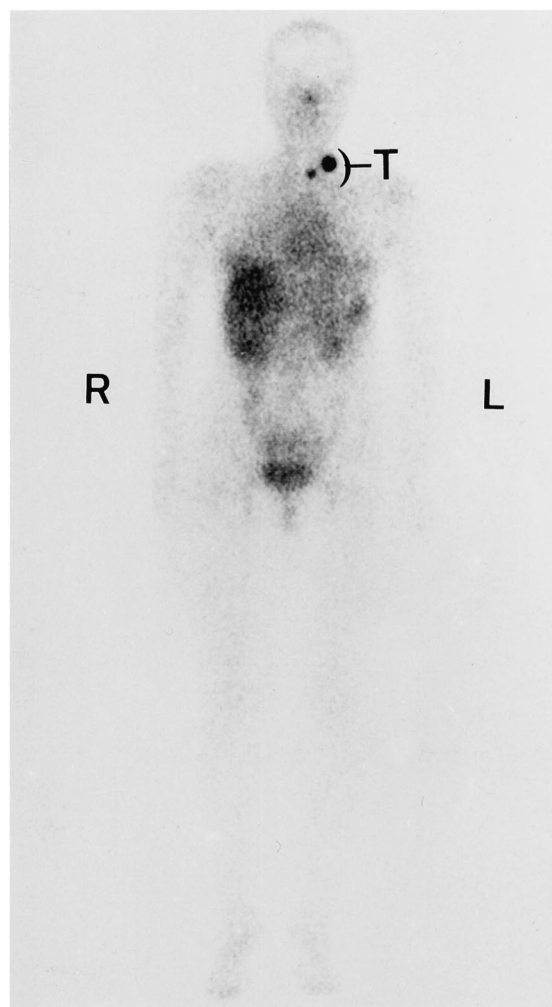


Fig. 1 AES immunoscintigraphy whole-body scan (anterior view, patient 3): detection in the neck area of two occult tumors (T), which had escaped conventional morphological imaging. Basal and stimulated calcitonin as well as CEA were restored to normal after surgery (30 months of follow-up).

rence detected by conventional imaging in patient 6 (right neck) corresponded to five distinct metastases detected by immunoscintigraphy: four were true positives, and one could not be found by the surgeon. Because circulating calcitonin was not restored to normal after surgery for this patient, we were unable to determine whether this location was a true or a false positive. Immunoscintigraphy disclosed two occult iliac bone metastases in patient 7, one mediastinal metastasis in patient 9, and in patient 10, there were two metastases at the right neck site: 1 pretracheal and 1 in the thorax. In the liver of patient 11, ultrasonography detected two metastases, and AES immunoscintigraphy disclosed more than eight foci accumulating activity; coelioscopy revealed the presence of numerous small metastatic nodules. Weak signals recorded in patients 6 (inflammatory site) and 12 corresponded to false-positive results.

**Weight of the Detected Metastases.** The smallest radioactive site detected by AES immunoscintigraphy corresponded



Table 3 Accuracy of RIGS (11 patients)

The operative field was explored with a hand-held gamma probe. A positive radioimmunoguided test was defined as greater than normal vicinal tissue counts plus twice the SD of normal tissue counts (*i.e.*, the square root of the counts). The hand-held gamma probe counts were recorded and compared with the results of anatomopathological examination.

Location	Size <sup>a</sup> (cm)	True-positive	True-negative	False-positive	False-negative	True/False
Lymph node	≥1	22	3	0	0	25/0
	>0.5	5	14	1	0	19/1
	≤0.5	16	85	8	13	101/21
Others <sup>b</sup>		3	32	4	2	35/6
Total ( <i>n</i> = 208)		46	134	13	15	

<sup>a</sup> Largest dimension of the tumor.

<sup>b</sup> Others are tissues free of lymph nodes.

to a tissue sample, weighing 360 mg. This sample contained a small tumor lymph node surrounded by connective tissue partially infiltrated with tumor cells.

### RIGS

RIGS was performed at  $3 \pm 1$  days after tracer injection, as described in "Patients and Methods." For each measurement, normal vicinal tissue was counted as a reference. The results of *in situ* gamma probe exploration for 208 locations (11 patients) are summarized in Table 3: 22.1% true positive, 64.4% true negative, 7.2% false negative, and 6.2% false positive. The accuracy was 86%, the sensitivity was 75%, and the specificity was 90%. Taking into account only the results concerning the lymph nodes >0.5 mm in diameter (*n* = 45), the accuracy was 98%, the sensitivity was 100%, and the specificity was 94%.

Of the 13 specimens giving false-positive results with *in situ* gamma probe detection, 9 were counted *ex vivo*. In four of nine cases of false-positive RIGS results (44%), no significant activity uptake was observed *ex vivo*; the false radioactive signal measured *in vivo* was attributable to blood vessels in the vicinity. In the five other cases, radioactivity accumulation was confirmed *ex vivo* and corresponded to non-tumor tissue with histiocytosis or fibrous reactions (56%). These specimens containing no tumor cells were of two kinds: two contained no CEA-expressing cells, but three contained histiocytes-macrophages that stained for CEA with a specific antibody, in agreement with the observations of Nabi *et al.* (23) for colorectal carcinoma (histiocytes-macrophages in other specimens were not stained for CEA).

The smallest detected metastatic lymph nodes were 0.2–0.3 cm in diameter (5–15 mg). Some were only partially infiltrated with tumor cells. A 0.1-mm-diameter metastasis located in a blood vessel was detected by RIGS (Fig. 2). In the surrounding tissue, an inflammatory reaction with numerous giant cells around a foreign body was detected by the pathologist. The giant cell macrophages present in the specimen were negative for CEA (in contrast to histiocytes-macrophages present in the three inflammatory false-positive lymph nodes described above). Because the tumor cells were located in a blood vessel, their accessibility to the bispecific antibody and the labeled hapten was high, and their radioactivity uptake might have been much higher than in less accessible tumor cells. We nevertheless cannot exclude that the observed accumulation of the radioactivity, allowing the detection of this very tiny tumor, was due to nonspecific uptake by macrophages.

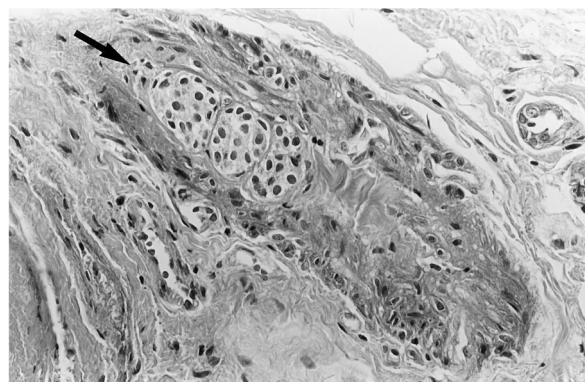


Fig. 2 This tumoral thrombosis located in a blood vessel was detected by RIGS (arrow). H&E, ×400.

The largest false-negatives were of the same mass as the smallest true-positives, 5–15 mg, except for two samples of 450 and 600 mg of conjunctivo-adipose tissue infiltrated with tumor cells. Both were attached to the jugular artery, and the circulating radioactivity was shielding the counts recorded by the hand-held gamma probe.

### Influence of HAMA on Immunoscintigraphy and RIGS in a Repeated Investigation

In one patient (no. 10), the control image obtained after the first surgery indicated the persistence of some radioactive sites. Two months later, another surgery was planned, and a second immunoscintigraphy was performed, although this patient had developed HAMA. No adverse effect was experienced by the patient. No site of activity uptake was imaged; nevertheless, RIGS detected six tumor lymph nodes of eight (tumor:muscle ratio,  $\geq 1.7$ ).

### Calcitonin and CEA Serum Level Follow-Up

Postsurgical calcitonin levels were normal (<10 pg/ml) or restored to normal for four patients (nos. 1, 2, 3, and 5) and remained normal for 30–42 months, whereas their serum calcitonin levels had ranged from 59 to 1135 pg/ml before surgery (Table 4). In two patients, the pentagastrin stimulation tests were normal 30 months after surgery (patients 1 and 3; test refused by patient 2). For one patient (no. 5), the calcitonin level was 33 pg/ml at  $t = 3$  min, in agreement with the presence of a

Table 4 Follow-up of serum calcitonin: basal and after pentagastrin stimulation

Patient no.	Serum Calcitonin (pg/ml) <sup>a</sup>			
	Basal			Pentagastrin stimulation
	Before surgery	4–10 days after surgery	Follow-up	
1	1135	<10	<10 (30 months)	Negative (30 months)
2	121	<10	<10 (34 months)	ND <sup>b</sup>
3	959	<10	<10 (30 months)	Negative (30 months)
4	548	257	338 (48 months)	ND
5	59	<10	<10 (42 months)	Peak, 33 pg/ml (4 months)
6	5671	790	1466 (38 months)	ND
7	4927 No surgery	ND	6178 (21 months)	ND
8	5993	1294	1703 (6 months)	ND
9	5035	1122	508 (22 months)	ND
10	695	306	692 (58 months)	ND
11	36073	ND	128600 (28 months)	ND
12	564	237	600 (34 months)	ND
13	343	275 (6 months)	475 (32 months)	ND

<sup>a</sup> Normal, <10 pg/ml.<sup>b</sup> ND, not done.

Table 5 Follow-up of circulating CEA

Patient no.	Before surgery <sup>a</sup> (ng/ml)	Postsurgery <sup>a</sup> (ng/ml)	Follow-up <sup>a</sup> (ng/ml)
1	32.8	<5	<5 (31 months)
2	91	<5	<5 (34 months)
3	10.8	<5	<5 (30 months)
4	10.3	<5	6.8 (48 months)
5	<5	<5	<5 (43 months)
6	6.9	<5	<5 (38 months)
7	82	No surgery	
8	56	22.1	19.8 (6 months)
9	131	41	17.7 (22 months)
10	26.4	<5	5.7 (58 months)
11	247	ND	565 (24 months)
12	20.7	ND	ND
13	17.7	ND	18.7 (4 months)

<sup>a</sup> Normal; <5 ng/ml.<sup>b</sup> ND, not done.

few residual tumor cells. CEA serum levels remained normal (<5 ng/ml) for these patients during the follow-up.

In five other patients (nos. 4, 6, 9, 10, and 12), calcitonin serum levels were lowered by 50% or more but not restored to normal, indicating the existence of residual disease (Table 4). For five of these patients, circulating calcitonin levels after 22–58 months of follow-up were lower than before surgery (nos. 4, 6, and 9) or similar (nos. 10 and 12). Follow-up of CEA serum level was performed for its elevation is indicative of poor prognosis (3, 14); it was restored to normal after surgery for patients 4, 6, and 10 (presurgery levels, 10.3, 6.9, and 26.4, respectively; Table 5). It remained normal for patient 6 and became slightly elevated for patients 4 and 10 at 38–58 months of follow-up. Patient 9's CEA level was considerably lowered after 22 months of follow-up (17.7 ng/ml, whereas the presurgery level was 131 ng/ml). Patient 13 had a tumor resection judged adequate by the surgeon but without significant decrease of calcitonin serum level. For patient 7, surgery was not performed because of the impossibility of removing the iliac bone

metastases. For two patients (nos. 8 and 11), a total resection of the known metastases was not feasible.

### Influence of AES Immunoscintigraphy and RIGS on Surgical Management

Immunoscintigraphy results altered the surgical approach for seven patients, with benefits for 5 of them (Table 6). The detection of occult metastases by immunoscintigraphy had the following consequences: decision to operate (no. 10) or to perform bilateral instead of monolateral surgery (no. 3), or to perform sternotomy (nos. 4 and 9). For one patient (no. 7), repeatedly operated before, whole-body immunoscintigraphy showed two unknown metastases on the iliac bone, confirmed by magnetic resonance imaging and histology on biopsy samples. Because the resection was not possible, the surgery planned to remove a neck metastasis was canceled. For two patients (nos. 6 and 12), AES immunoscintigraphy visualized every metastases, but an additional signal was a false positive.

RIGS allowed the resection of additional pathological lymph nodes in six patients (Table 6). For four of these patients (nos. 4, 6, 9, and 10), surgery was considered complete according to RIGS, but the calcitonin serum levels were not restored to normal, indicating the persistence of residual disease.

For two patients (nos. 3 and 5), CEA and basal CT levels were normalized. Immunoscintigraphy detected two occult metastases in patient no. 3 (Fig. 1); one, which escaped bilateral lymphadenectomy, was removed thanks to RIGS. The pentagastrin test was still negative 30 months after surgery. In patient 5, the RIGS signal led to the removal of a 2-mm tumor lymph node. Basal serum calcitonin of this patient remained normal 42 months after surgery.

### DISCUSSION

Efficacy of classical immunoscintigraphy and RIGS is frequently limited by low tumor:normal tissue ratios. Preliminary clinical studies have shown the feasibility of AES for detecting colorectal carcinoma (24, 25), MTC (18, 19, 26), and non-small cell lung cancer (27) and have demonstrated that AES improves

Table 6 AES immunoscintigraphy and RIGS influence on surgical management

Patient no.	Immunoscintigraphy	RIGS
1	No change	No change
2	No change	No change
3	+++ Occult metastases detected, sternotomy decided	++++ Small tumor lymph node detected by RIGS and resected. CT normalization.
4	+++ Occult metastases detected, sternotomy decided	+ More complete surgery. Persistence of the disease.
5	No change	+++ Unknown small tumor lymph node detected by RIGS and resected. CT normalization.
6	Second unnecessary surgery (false-positive inflammatory site on postoperative images)	+
7	++++	Not done.
8	total resection not feasible No change	No change
9	+++ Occult metastases detected, sternotomy decided	+ More complete surgery. Persistence of the disease.
10	Surgery decided	+ More complete surgery. Persistence of the disease.
11	Total resection not feasible. No change. visualization of multiple hepatic metastases.	No change
12	Right side unnecessary dissection	No change
13	No change	No change

tumor:normal tissue ratios (17, 24) compared with classical immunoscintigraphy with directly labeled antibody fragments or pretargeted monovalent haptens (28).

Although the hapten circulated as a complex with the bispecific antibody, its initial decline in the circulation was fast because of the rapid clearance of the unbound fraction in the urine. As a consequence, tumor:normal tissue ratios increased rapidly, 24 h after hapten administration being the optimal time for immunoscintigraphy. Tumor uptake was stable, and thus tumor:nontumor contrast ratios kept increasing over time, and this has been useful in a few cases where imaging at later times has allowed us to detect additional tumor sites. It also made RIGS possible up to 7 days after hapten administration.

The results presented here have been confirmed by pathological examination of surgical or biopsy samples or selective venous catheterization. The technique is very sensitive given that, of 34 metastases detected by AES immunoscintigraphy, 22 escaped classical preoperative imaging. High-contrast images were obtained in most cases and indicated that two successive injections 4 days apart (one of the bispecific antibody, the other of the labeled bivalent hapten) greatly enhanced diagnostic reliability. One patient received a second administration of the AES reagents while she was HAMA positive. The presence of HAMA did not cause any clinical problem but definitely decreased targeting efficiency (25).

The benefit of AES immunoscintigraphy for the patients was illustrated by the influence of immunoscintigraphy on the efficacy of surgery. It was clearly demonstrated in one of the four patients (nos. 3, 4, 9, and 10), operated on because immunoscintigraphy detected occult tumors; patient 3 had his serum calcitonin and CEA restored to normal. In addition, the time to progression may have been delayed in the other cases (nos. 4, 9, and 10), in which a large decrease in circulating CEA, an important prognostic factor (3, 14), was achieved. CEA was

restored to normal for two of these patients after surgery and remained below presurgery level 22–58 months later for the three (Table 5). Finally, whole-body scanning allowed the detection of distant metastases, which represents a major advantage of the present approach. In one patient, two occult iliac bone foci, out of surgical reach, were visualized by immunoscintigraphy. Cancellation of a useless surgery was an appreciated benefit for this patient, in agreement with the earlier observation of Juweid *et al.* (29).

Improved sensitivity and specificity of tumor imaging translated into better clinical management. Surgery may often be only palliative in MTC recurrences, when tumor resection is not complete, as shown by the absence of normalization of serum calcitonin (4, 6). This explains the decision to operate, even with marginally significant immunoscintigraphy indications. False-positive immunoscintigraphy interpretation could probably be minimized with a longer practice of the technique. In addition, we cannot exclude that some of these marginally significant images were attributable to very small positive lymph nodes not found by the surgeon.

Localization of tumors by their activity uptake provided a major surgical opportunity. RIGS allowed us to detect very small tumors, including those too small to be detected by immunoscintigraphy. The efficacy of the present technique was established because 16 detected pathological lymph nodes were 0.2–0.3 cm in diameter. In six cases, RIGS allowed resection of tumor sites that otherwise would have escaped surgery, and serum calcitonin was restored to normal ( $\leq 10$  pg/ml) in two patients (patients 3 and 5).

MTC is a rare disease; the number of patients investigated thus far ruled out statistical treatment. AES immunoscintigraphy, followed by RIGS, enabled us to remove occult metastases with a benefit for six patients, including two patients in which basal calcitonin was restored to normal (follow-up, 30 and 52

months), and for one of these, the normalization of the penta-gastrin-stimulated calcitonin. In the absence of RIGS, only very extensive surgery ("microsurgery") achieves calcitonin normalization in a significant number of occult metastatic MTC (2, 30–32), but the surgical technique is more difficult, and complications are greater than conventional surgery (3). Therefore, the approach of most experienced centers is a more conservative palliative treatment for recurrent MTC (3).

In conclusion, AES immunoscintigraphy and RIGS allow the resection of very small unanticipated tumors. They are new and powerful tools for the conventional surgical management of patients in recurrent MTC, primarily for occult recurrent MTC. In addition they might be of valuable help for the "microdissection" surgical approach. Only very small lesions may escape both. In such cases, AES radioimmunotherapy after RIGS may become the treatment of choice.

## ACKNOWLEDGMENTS

We gratefully acknowledge the help and suggestions of Professor A. A. Benson (University of California San Diego) during the revision of the manuscript.

## REFERENCES

- Rossi, R. L., Cady, B., Meissner, W. A., Wool, M. S., Sedgwick, C. E., and Werber, J. Non familial medullary thyroid carcinoma. *Am. J. Surg.*, 139: 554–560, 1980.
- Buhr, H. J., Kallinowski, F., Raue, F., Frank-Raue, K., and Herfarth, C. Microsurgical neck dissection for occultly metastasizing medullary thyroid carcinoma three year results. *Cancer (Phila.)*, 72: 3685–3693, 1993.
- Heshmati, H. M., Gharib, H., van Heerden, J. A., and Sizemore, G. W. Advances and controversies in the diagnosis and management of medullary thyroid carcinoma. *Am. J. Med.*, 103: 60–69, 1997.
- Jackson, C. E., Talpos, G. B., Kambouris, A., Yott, J. B., Tashjian, A. H., and Block, M. A. The clinical course after definitive operation for medullary thyroid carcinoma. *Surgery*, 94: 995–1001, 1983.
- Gharib, H., McCohaney, W. M., Tieg, R. D., Bergstralh, E. J., Goellner, J. R., Grant, C. S., van Heerden, J. A., Sizemore, G. W., and Hay, I. D. Medullary thyroid carcinoma: clinicopathologic features and long-term follow-up of 65 patients treated during 1946 through 1970. *Mayo Clin. Proc.*, 67: 934–940, 1992.
- Tisell, L. E., Hansson, G., Jansson, S., and Salander, H. Reoperation in the treatment of asymptomatic metastasizing medullary thyroid carcinoma. *Surgery*, 99: 60–66, 1986.
- van Heerden, J. A., Grant, C. S., Gharib, H., Hay, I. D., and Ilstrup, D. M. Long term course of patients with persistent hypercalcitonemia after apparent curative primary surgery for medullary thyroid carcinoma. *Ann. Surg.*, 212: 395–401, 1990.
- Milhaud, G., Tubiana, M., Parmentier, C., and Coutris, G. Epithelioma de la thyroïde sécrétant de la thyrocalcitonine. *C. R. Acad. Sci.*, 266: 608–610, 1968.
- Calmettes, C., Moukhtar, M. S., and Milhaud, G. Plasma carcinoembryonic antigen *versus* plasma calcitonin in the diagnosis of medullary carcinoma of the thyroid. *Cancer Immunol. Immunother.*, 4: 251–256, 1978.
- Goltzman, D., Potts, J. T., Ridgway, E. C., and Maloof, F. Calcitonin as a tumor marker. Use of the radioimmunoassay for calcitonin in the postoperative evaluation of patients with medullary thyroid carcinoma. *N. Engl. J. Med.*, 290: 1035–1039, 1974.
- Block, M. A., Jackson, C. E., and Tashjian, A. H., Jr. Management of occult medullary thyroid carcinoma evidenced only by serum calcitonin level elevations after apparently adequate neck operations. *Arch. Surg.*, 113: 368–372, 1978.
- Calmettes, C., Ponder, B. A. J., Fischer, J. A., Raue, F., and the members of the European Community Concerted Action. Medullary thyroid carcinoma. Early diagnosis of the multiple endocrine neoplasia type 2 syndrome: consensus statement. *Eur. J. Clin. Investig.*, 22: 755–760, 1992.
- Gharib, H., Kao, P. C., and Heath, H., III. Determination of silica purified plasma calcitonin for the detection and management of medullary thyroid carcinoma: comparison of two provocative tests. *Mayo Clin. Proc.*, 62: 373–378, 1987.
- Mendelsohn, G., Wells, S. A., Jr., and Baylin, S. B. Relationship of tissue carcinoembryonic antigen and calcitonin to tumor virulence in medullary thyroid carcinoma. An immunohistochemical study in early, localized, and virulent disseminated stages of disease. *Cancer (Phila.)*, 54: 657–662, 1984.
- O'Byrne, K. J., Hamilton, D., Robinson, I., Sweeney, E., Freyne, P. J., and Cullen, M. J. Imaging of medullary carcinoma of the thyroid using <sup>111</sup>In-labelled anti-CEA monoclonal antibody fragments. *Nucl. Med. Commun.*, 13: 142–148, 1992.
- Juweid, M., Sharkey, R. M., Behr, T., Swaine, L. C., Herskovic, T., Pereira, M., Rubin, A. D., Hanley, D., Dunn, R., Siegel, J., and Goldenberg, D. M. Radioimmunotherapy of medullary thyroid cancer with iodine-131-labeled anti-CEA antibodies. *J. Nucl. Med.*, 37: 905–911, 1996.
- Le Doussal, J. M., Gruaz-Guyon, A., Martin, M., Gautherot, E., Delaage, M., and Barbet, J. Targeting of indium-111-labeled bivalent hapten to human melanoma mediated by bispecific monoclonal antibody conjugates: imaging of tumors hosted in nude mice. *Cancer Res.*, 50: 3445–3452, 1990.
- de Labriolle-Vaylet, C., Wioland, M., Sarfati, E., Béranger, N., Billotey, C., Chigot, J. P., Meyer, P., Barbet, J., Milhaud, G., Mensch, S., Askienazy, S., Gruaz-Guyon, A., *et al.* Radioimmunodetection de métastases du cancer médullaire de la thyroïde (CMT) à l'aide d'une nouvelle méthode en deux temps. *Med. Nucl.*, 7/8: 318, 1993.
- Peltier, P., Curtet, C., Chatal, J. F., Le Doussal, J. M., Daniel, G., Aillet, G., Gruaz-Guyon, A., Barbet, J., and Delaage, M. Radioimmunodetection of medullary thyroid cancer using a bispecific anti-CEA/anti-In-DTPA antibody and an indium-111-labeled DTPA dimer. *J. Nucl. Med.*, 34: 1267–1273, 1993.
- Janevik-Ivanovska, E., Gautherot, E., Hillairet de Boisferon, M., Cohen, M., Milhaud, G., Tartar, A., Rostene, W., Barbet, J., and Gruaz-Guyon, A. Bivalent hapten-bearing peptides designed for iodine-131 pretargeted radioimmunotherapy. *Bioconjugate Chem.*, 8: 526–533, 1997.
- Augereau, B., Wioland, M., de Labriolle-Vaylet, C., Padovani, J. P., Martin, T., Verneret, C., Apoil, A., and Milhaud, G. Le repérage isotopique per-opérateur des ostéomes ostéoïdes et autres lésions hyperfixantes à la scintigraphie. *Rev. Chir. Orthop.*, 74: 764–770, 1988.
- Wioland, M., and Sergent-Alaoui, A. Didactic review of 175 radionuclide-guided excisions of osteoid osteomas. *Eur. J. Nucl. Med.*, 23: 1003–1011, 1996.
- Nabi, H. A., Doerr, R. J., Balu, D., Rogan, L., Farrell, E. L., and Evans, N. H. Gamma probe assisted *ex vivo* detection of small lymph node metastases following the administration of indium-111-labeled monoclonal antibodies to colorectal cancers. *J. Nucl. Med.*, 34: 1818–1822.
- Le Doussal, J. M., Chetanneau, A., Gruaz-Guyon, A., Martin, M., Gautherot, E., Lehur, P. A., Chatal, F., Delaage, M., and Barbet, J. Bispecific monoclonal antibody-mediated targeting of an indium-111-labeled DTPA dimer to primary colorectal tumors: pharmacokinetics, biodistribution, scintigraphy and immune response. *J. Nucl. Med.*, 34: 1662–1671, 1993.
- Chetanneau, A., Barbet, J., Peltier, P., Le Doussal, J. M., Gruaz-Guyon, A., Bernard, A. M., Resche, I., Rouvier, E., Bourguet, P., Delaage, M., and Chatal, F. Pretargeted imaging of colorectal cancer recurrences using an <sup>111</sup>In-labelled bivalent hapten and a bispecific antibody conjugate. *Nucl. Med. Commun.*, 15: 972–980, 1994.



26. Barbet, J., Peltier, P., Bardet, S., Vuillez, J. P., Bachelot, I., Denet, S., Olivier, P., Leccia, F., Corcuff, B., Huglo, D., Proye, C., Rouvier, E., Meyer, P., and Chatal, F. Radioimmunodetection of medullary thyroid carcinoma using indium-111 bivalent hapten and anti-CEA x anti-DTPA-Indium bispecific antibody. *J. Nucl. Med.*, 39: 1172–1178, 1998.
27. Vuillez, J. P., Moro, D., Brichon, P. Y., Rouvier, E., Brambilla, E., Barbet, J., Peltier, P., Meyer, P., Sarrazin, R., and Brambilla, C. Two-step immunoscintigraphy for non-small cell lung cancer staging using a bispecific anti-CEA/anti-indium-DTPA antibody and an indium-111-labeled DTPA dimer. *J. Nucl. Med.*, 38: 507–511, 1997.
28. Stickney, D. R., Anderson, L. D., Slater, J. B., Ahlem, C. N., Kirk, G. A., Schweighardt, S. A., and Frincke, J. M. Bifunctional antibody: a binary radiopharmaceutical delivery system for imaging colorectal carcinoma. *Cancer Res.*, 51: 6650–6655, 1991.
29. Juweid, M., Sharkey, R. M., Swayne, L. C., and Goldenberg, D. M. Improved selection of patients for reoperation for medullary thyroid cancer by imaging with radiolabeled anticarcinoembryonic antigen antibody. *Surgery*, 122: 1156–1165, 1997.
30. Moley, J. F., Wells, S. A., Dilley, W. G., and Tisell, L. E. Reoperation for recurrent or persistent medullary thyroid cancer. *Surgery*, 114: 1090–1095, 1993.
31. Moley, J. F., Debenedetti, M. K., Dilley, W. G., Tisell, L. E., and Wells, S. A. Surgical management of patients with persistent or recurrent medullary thyroid cancer. *J. Int. Med.*, 243: 521–526, 1998.
32. Tisell, L. E., Dilley, W. G., and Wells, S. A. Progression of post-operative residual medullary thyroid carcinoma as monitored by plasma calcitonin levels. *Surgery*, 119: 34–35, 1996.